

# Measurements of Radiation Doses Induced by High Intensity Laser between $10^{16}$ and $10^{21}$ W/cm<sup>2</sup> onto Solid Targets at LCLS MEC Instrument

T. Liang<sup>1,2</sup>, J. Bauer<sup>1</sup>, M. Cimen<sup>1</sup>, A. Ferrari<sup>3</sup>, E. Galtier<sup>1</sup>, E. Granados<sup>1</sup>, P. Heimann<sup>1</sup>, H. J. Lee<sup>1</sup>, J. Liu<sup>1</sup>, D. Milanthianaki<sup>1</sup>, B. Nagler<sup>1</sup>, A. Prinz<sup>1</sup>, S Rokni<sup>1</sup>, H. Tran<sup>1</sup> and M. Woods<sup>1</sup>

<sup>1</sup>SLAC National Accelerator Laboratory, 2757 Sand Hill Rd, Menlo Park, CA 94025 USA

<sup>2</sup>Georgia Institute of Technology, North Ave NW, Atlanta, GA 30332 USA

<sup>3</sup>HZDR Institute of Radiation Physics, Bautzner Landstraße 400, 01328 Dresden, Germany

## Abstract

The Radiation Protection (RP) group at SLAC National Accelerator Laboratory performed systematic and comprehensive measurements with various active and passive detectors for high intensity lasers (between  $10^{16}$ - $10^{21}$  W/cm<sup>2</sup>) focused onto thin solid metal targets at LCLS Matter in Extreme Conditions (MEC) instrument. Laser scientists at MEC characterized the laser and optics parameters for each measurement. Outside the target chamber, photon doses were detected starting at  $3 \times 10^{16}$  W/cm<sup>2</sup> and neutron doses starting at  $6 \times 10^{17}$  W/cm<sup>2</sup>. SLAC RP developed a photon dose yield model to perform hazard analysis, establish controls, and calculate shielding for laser-matter experiments at MEC and a future petawatt (PW) laser facility at SLAC.

## 1. Introduction

The number and use of high power multi-terawatt and petawatt lasers for different applications continues to increase around the world. Laser-matter interactions are used for different applications including the study of matter under extreme conditions<sup>[1]</sup>, the production of energetic beams of protons and/or electrons<sup>[2][3]</sup>, and the generation forward-directed betatron X-rays<sup>[4][5]</sup>. These interactions are a source of ionizing radiation and require radiological safety measures, including shielding, interlocked access control and radiation monitoring, to protect personnel. This paper presents the radiation measurement results, the photon dose yield model developed, the shielding attenuation calculations, and some preliminary results of studies on electron spectrometry and hot electron source terms.

## 2. SLAC RP Dose Yield Model and Measurements

SLAC RP's original photon dose yield model was presented before<sup>[6][7]</sup>. Figure 1 shows the SLAC RP *adjusted* dose yield model at 1 meter in the 0° laser forward direction as a function of laser intensity (with  $\lambda = 0.8 \mu\text{m}$ ) with and without the 2.54-cm-thick Al-wall attenuation. The measurement data taken at MEC and at LLNL's Titan<sup>[8]</sup> are plotted in the figure. The data provided by U.K. RAL is also shown for comparison.

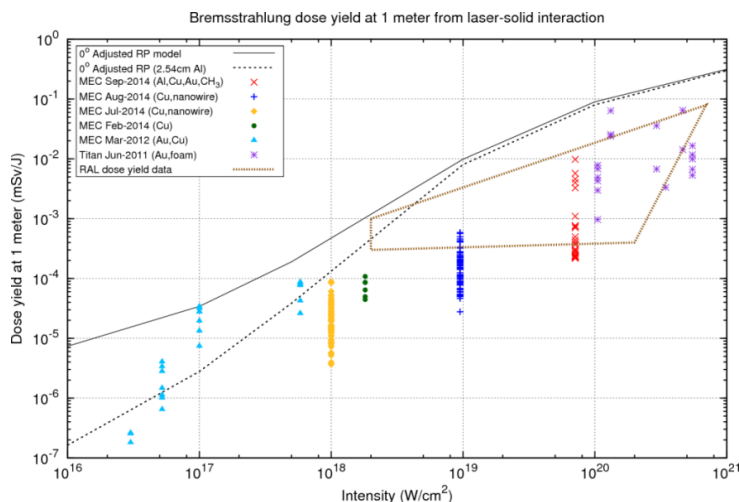


Figure 1 – Complete measurement data for  $10^{16}$ - $10^{21}$  W/cm<sup>2</sup> with adjusted 0° RP dose yield model. There were no measurements taken at 0° during MEC Sep-2014 due to the presence of a tungsten shield in the forward direction.

The dose yield data for each experiment is spread over about an order of magnitude because detectors/dosimeters were deployed at various angles and saw different levels of shielding by the Al target chamber. The original RP model (not plotted in the figure) was adjusted based on SLAC RP measurements. The adjusted dose yield model agrees with the maximum values from measurements but overestimates by a factor of 10 at  $10^{19}$  W/cm<sup>2</sup>. For  $7 \times 10^{19}$  W/cm<sup>2</sup>, the maximum dose yields were measured at 90° because tungsten shielding in the laser forward direction blocked the measurements at 0°, but it is predicted that if there were unshielded measurements in the 0° forward direction, those measurements would agree well with the dose yield curves. The 0° adjusted RP model (with 2.54 cm Al shielding) is reasonably conservative and is used by SLAC to estimate dose hazards and shielding requirements for laser-metal interactions at MEC.

### 2.1. Active and Passive Detector Performance

The response of active detectors may be affected at high laser intensity. Evidence of this was seen during the measurements at LLNL's Titan<sup>[8]</sup>, in which all active detectors were reading zero or much lower.

Figure 2 shows a comparison of photon deep dose measured by several passive and active detectors during the Titan experiment for single laser shots between  $10^{20}$ - $10^{21}$  W/cm<sup>2</sup> onto thin CH foam and Au foil. The response of passive Panasonic TLD, Luxel+ OSLD, and pocket ion chamber (PIC) dosimeters agree well. On the other hand, the active Victoreen 450 handheld ion chamber instrument under responded by about a factor of 10 compared to the passive detectors. This may be due to the high EMP or high instantaneous pulsed radiation fields generated from single high-intensity and high-energy laser shots at Titan or from the Victoreen's software being unable to handle radiation from short pulses.

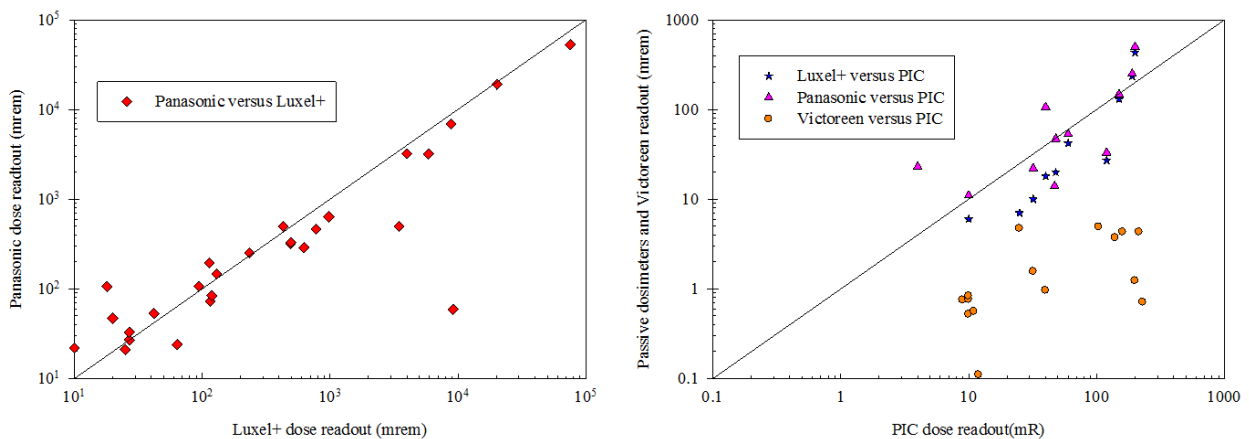


Figure 2 – Comparison of photon deep dose measured by several active and passive detectors at LLNL Titan.

### 3. Shielding Tenth Value Layer (TVL)

The Tenth Value Layer (TVL) thicknesses of the materials [concrete, stainless steel 304 (SS304), and lead] needed to attenuate a Maxwellian-shape bremsstrahlung spectrum generated by hot electrons originating from laser-solid interactions were calculated<sup>[9]</sup> using FLUKA Monte Carlo code<sup>[10][11]</sup>. Figure 3 provides TVLs for concrete and SS304, and Figure 4 for lead. TVL<sub>1</sub> is the thickness of the first TVL layer, and TVL<sub>2</sub> is the thickness of the second TVL. Since TVL<sub>3</sub> was found to be equivalent to TVL<sub>2</sub>, TVL<sub>2</sub> can also be called the equilibrium TVL (TVL<sub>e</sub>), where all additional TVL layers are the same thickness. The TVL values were found to be in good agreement as those reported in NCRP Report No. 144.

These TVL values are used in shielding design at high intensity laser facilities at SLAC. Currently MEC utilizes a combination of metal local shielding inside the target chamber and moveable Pb panels outside the chamber, because the thin lead hutch walls were designed originally for LCLS FEL operations only.

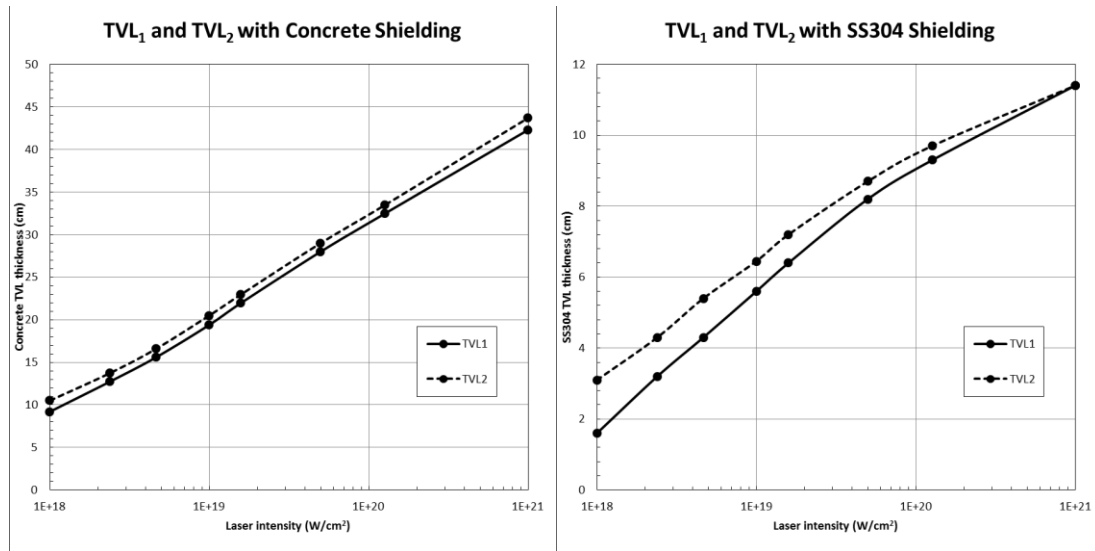


Figure 3 – Tenth value layers for concrete and SS304 calculated with FLUKA from Maxwellian photon spectra.

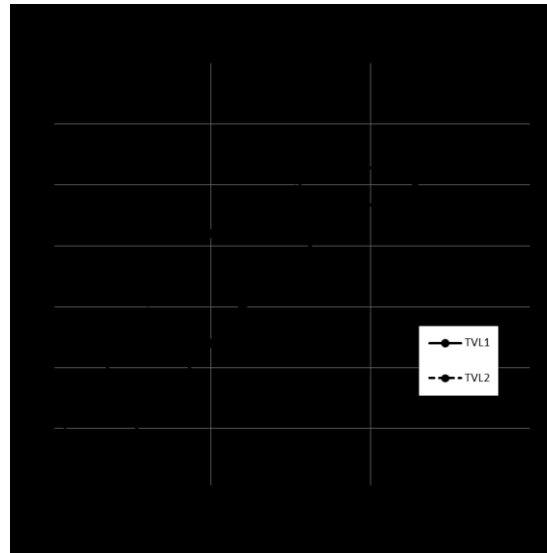


Figure 4 – Tenth value layers for lead calculated with FLUKA from Maxwellian photon spectra

#### 4. Preliminary Work on Spectrometry and Electron Source Terms

A possible reason for the overestimation of the RP dose yield model, particularly at  $10^{19}$  W/cm<sup>2</sup>, may be due to hot electron energy spectrum model used. The spectra of electrons and photons inside target chamber during MEC laser-solid experiments were measured to evaluate hot electron energy spectrum information (and subsequent bremsstrahlung spectrum). The measured depth-dose curves are obtained from spectrometers constructed of alternating layers of attenuating material (plastic for electrons and aluminum for photons) and passive Landauer nanoDot dosimeters (aluminum oxide detector). Figure 5 presents preliminary results from spectrometry measurements from a MEC experiment with laser of  $10^{19}$  W/cm<sup>2</sup> onto 100  $\mu$ m Cu foils.

Figure 5 also shows that FLUKA simulations with a Maxwellian electron spectrum (characterized by a hot electron temperature  $T_h$  of 0.70 MeV) generates a relative electron depth-dose curve that agrees better with the measured curves than a relativistic Maxwellian electron spectrum (characterize by the same  $T_h$ ).

Simulations with a particle-in-cell (PIC) code <sup>[9]</sup> can help further explore the hot electron parameters (yield, energy and angular distributions) generated by the interaction of a high-intensity laser with plasma. Figure 6 shows a Maxwellian curve fitted better to the hot electron spectrum calculated with a PIC code simulation for laser of  $10^{19}$  W/cm<sup>2</sup> hitting 100  $\mu$ m Cu foils.

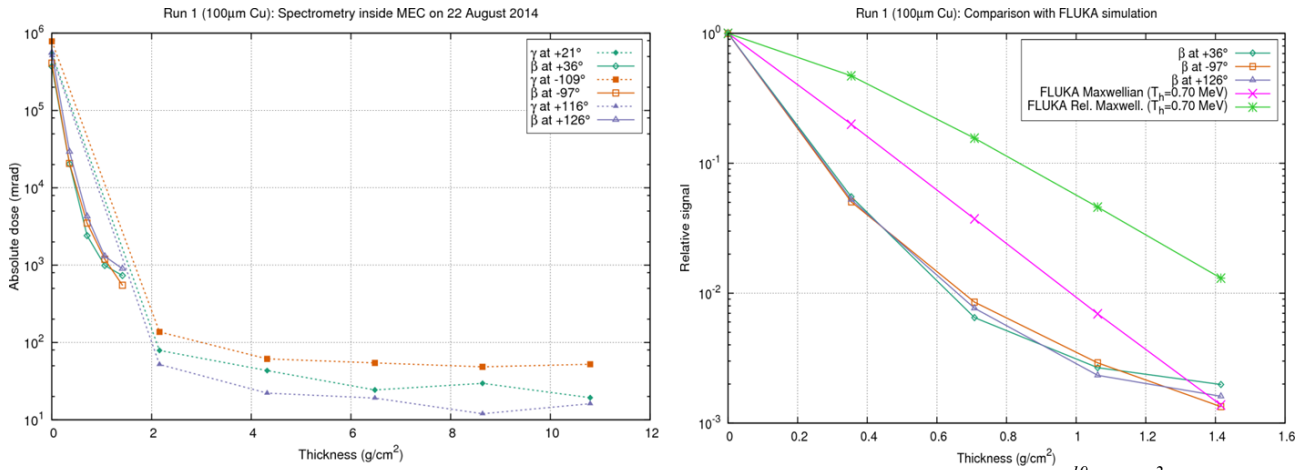


Figure 5 – Preliminary spectrometry results from laser-solid experiment at MEC for  $10^{19}$  W/cm<sup>2</sup>.

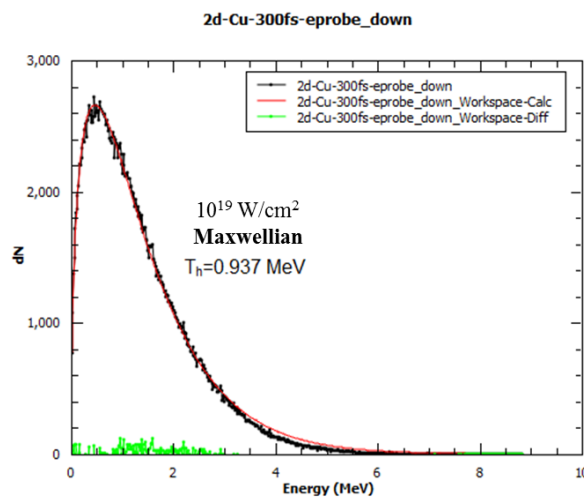


Figure 6 – Maxwellian hot electron distribution for  $10^{19}$  W/cm<sup>2</sup> calculated by PIC code. The ponderomotive formula gives  $T_h = 0.70$  MeV.

The above measurements and FLUKA calculations for electron depth doses, as well as the PIC calculations for electron spectrum, indicate that RP model (a relative Maxwellian spectrum model) may not be correct at  $10^{19}$  W/cm<sup>2</sup>. Future work will pair the hot electron and angular distributions generated from PIC code with the electron transport and radiation calculation capability of FLUKA. Comparing these calculations with the SLAC electron spectrometry results presented earlier will then help refine both the hot electron source term and the photon dose yield model for high-intensity laser-solid interactions.

## 5. Summary

In the last few years, systematic and comprehensive measurements of ionizing radiation yields from laser-solid interactions have been conducted for intensities between  $10^{16}$ - $10^{20}$  W/cm<sup>2</sup> at MEC and between  $10^{20}$ - $10^{21}$  W/cm<sup>2</sup> at LLNL. Passive and active detectors were used and their performance in this type of radiation fields was examined. Laser and optics parameters were well characterized in order to correlate with dose results. These efforts contributed to the development of an adjusted photon dose yield model that allows SLAC RP to evaluate the dose hazards, develop radiological controls<sup>[9]</sup>, and set shielding requirements for high-intensity laser-solid experiments at MEC and at the future SLAC petawatt laser facility.

## References

- [1] L. B. Fletcher *et al.*, “Ultrabright X-ray laser scattering for dynamic warm dense matter physics”, *Nat. Photonics* **9**, 274-279 (2015).
- [2] W. P. Leemans *et al.*, “GeV electron beams from a centimeter-scale accelerator”, *Nat. Phys.* **2**, 696-699 (2006).

- [3] S. Fourmaux *et al.*, “Investigation of laser-driven proton acceleration using ultra-short, ultra-intense laser pulses”, *Phys. Plasmas* **20**, 013110 (2013).
- [4] F. Albert *et al.*, “Angular Dependence of Betatron X-ray Spectra from a Laser-Wakefield Accelerator”, *Phys. Rev. Lett.* **111**, 235004 (2013).
- [5] L. M. Chen *et al.*, “Bright betatron X-ray radiation from a laser-driven-clustering gas target”, *Scientific Reports* **3**, 1-5 (2013).
- [6] R. Qiu *et al.*, “Analysis and mitigation of x-ray hazard generated from high intensity laser-target interactions”, *SLAC Publications SLAC PUB-14351*, 1-9 (2011).
- [7] T. Liang *et al.*, “Measurements of high-intensity laser induced ionizing radiation at SLAC”, *Shielding Aspects of Accelerators, Targets and Irradiation Facilities SATIF-12 Workshop Proceedings*, 40-53 (2015).
- [8] J. Bauer *et al.*, “High Intensity Laser Induced Radiation Measurements at LLNL”, *SLAC Radiation Physics Note*, RP-11-11 (2011).
- [9] T. Liang and J. Liu, “TVL Values of Common Shielding Materials for Bremsstrahlung from MEC Laser Operations”, *SLAC Radiation Physics Note*, RP-13-20 (2014).
- [10] “The FLUKA code: Description and benchmarking” G. Battistoni, S. Muraro, P.R. Sala, F. Cerutti, A. Ferrari, S. Roesler, A. Fassò, J. Ranft, *Proceedings of the Hadronic Shower Simulation Workshop 2006*, Fermilab 6-8 September 2006, M. Albrow, R. Raja eds., *AIP Conference Proceeding* 896, 31-49, (2007).
- [11] “FLUKA: a multi-particle transport code” A. Fassò, A. Ferrari, J. Ranft, and P.R. Sala, *CERN-2005-10* (2005), *INFN/TC\_05/11*, *SLAC-R-773*.
- [12] “EPOCH: the Extendable PIC Open Collaboration project to develop a UK community advanced relativistic EM PIC code.”
- [13] J. Bauer *et al.*, these proceedings.